

# Transient Heat Flux Measurements in a Divided-Chamber Diesel Engine

*Transient surface heat flux measurements were performed at several locations on the cylinder head of a divided-chamber diesel engine. The local heat flux histories were found to be significantly different. These differences are attributed to the spatial nonuniformity of the fluid motion and combustion. Both local time averaged and local peak heat fluxes decreased with decreasing speed and load. Retarding the combustion timing beyond TDC decreased the peak heat flux in the antechamber but increased the peak heat flux in the main chamber. This is attributed to the relative increase in the portion of fuel that burns in the main chamber with retarded combustion timing.*

## Introduction

Despite a relatively large number of studies dealing with transient heat transfer in open-chamber diesel engines [1-7], corresponding investigations in divided-chamber diesel engines have been very few [8-10]. Of these, Knight [8] presented very limited data, and Hassan [9] investigated only motored conditions in an experimental, low-compression ratio, divided-chamber engine with spherical antechamber geometry. Kamel [10] (see also Kamei and Watson [11]), on the other hand, performed a detailed study of transient heat transfer in a high-swirl, divided-chamber engine. Heat flux measurements were made at a location in the antechamber (hot plug) and at a location in the main chamber. The engine variables examined were engine speed (1320 to 2800 r/min), load (100 and 40 percent) and injection timing (2°, 7°, and 12° BTDC).

The objectives of this investigation were twofold: first, to obtain time-resolved, surface heat flux measurements at several locations on the cylinder head of a divided-chamber diesel engine, and second, to examine the influence of the principal operational parameters of the engine on the local heat flux histories.

## Apparatus and Procedure

**Engine.** The heat flux measurements were performed in a 0.72-L experimental, single-cylinder, divided-chamber diesel engine. The characteristic dimensions of the engine are given in Table 1. The cylinder head was specially designed to allow the introduction of four heat flux probes and two pressure transducers. Two of the probes, designated as TM1 and TM2, were located in the main chamber, and the other two probes, designated as TS1 and TS2, were located in the antechamber. The locations of the probes relative to the valves, cylinder, and antechamber are shown in Fig. 1. Of the two main chamber probes, TM1 was located between the valves and in line with the antechamber passage, and TM2 was located near the periphery of the cylinder and to the side of the throat. Both of the antechamber probes, TS1 and TS2, were located in the upper half of the antechamber. Probe TS1 was in the Plane containing the fuel injector and the centerline of the connecting passage (see section AA, Fig. 1). The location TS2 was used for limited tests only.

**Heat Flux Probes.** The heat flux probes were fast-response, surface thermocouples of the Bendersky type [12]

Contributed by the Heat Transfer Division for publication in the JOURNAL OF HEAT TRANSFER. Manuscript received by the Heat Transfer Division April 6, 1984.

Table 1 Engine description

Bore, mm	103.0
Stroke, mm	85.6
Connecting rod length, mm	223.5
Displacement, L	0.718
Antechamber volume, L	0.0147
Compression ratio	19.2:1
Intake valve opens, CA deg	6 BTC
Intake valve closes, CA deg	38 ABC
Exhaust valve opens, CA deg	64 BBC
Exhaust valve closes, CA deg	17 ATC

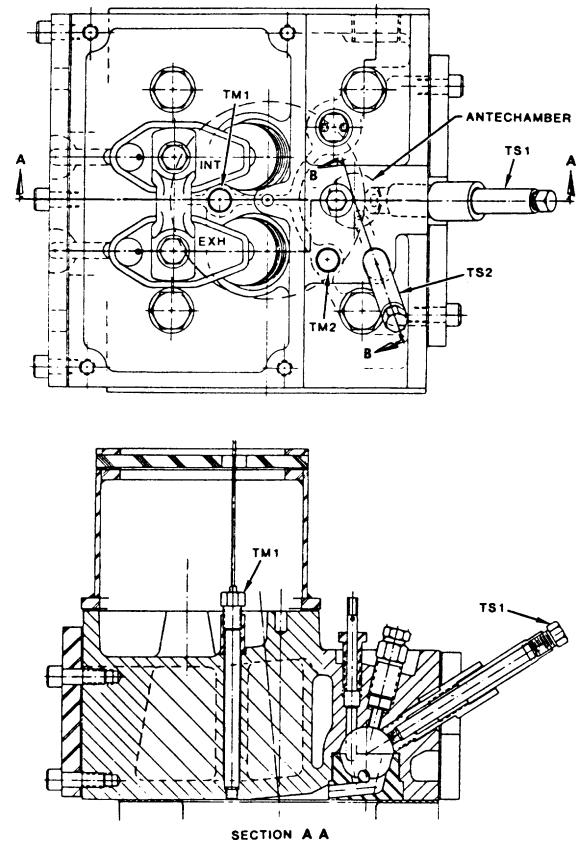


Fig. 1 Locations of heat flux probes on the cylinder head

with a second thermocouple placed at a nominal distance of 13 mm from the tip of the probe. The probe bodies were manufactured from the same material used in making the

**Table 2 Baseline conditions**

Engine speed, r/min	1000
Fuel-air ratio	0.022
Start of combustion	TDC
Intake-air temperature, °C	35
Coolant temperature, °C	82
Intake-air manifold pressure	ambient
Oil temperature, °C	82
Fuel temperature at pump, °C	35

cylinder head. The diameter of the tip of the probe was 6.4 trim. The surface thermocouples have a response time of the order of 1 to 10  $\mu$ s. The second thermocouple ("in-depth" thermocouple) was used to measure the time-averaged component of heat flux  $q$ , which is given by the following expression

$$q_w = \frac{K}{\delta} [T(0) - T(\delta)] \quad (1)$$

where  $K$  is the thermal conductivity of the probe material,  $\delta$  is the distance of the "in-depth" thermocouple from the surface of the probe, and  $T(0)$  and  $T(\delta)$  are the time-averaged temperatures at the surface ( $x = 0$ ) and at a distance  $x = \delta$  from the surface.

The heat flux probes were calibrated in a separate calibration rig which consisted of a water-cooled, high-intensity radiation source (36 kW), a reference heat flux sensor (Hy-Cal asymptotic water-cooled calorimeter), and a holder where the heat flux probe to be calibrated is mounted. The mounting of the heat flux probes in the holder was identical to the mounting of the probes in the cylinder head. The magnitude of the incident radiant heat flux to the probe was measured by the calorimeter. The surface absorptivity of the calorimeter ( $a = 0.89$ ) was assumed to be approximately equal to the surface absorptivity of the heat flux probes whose surfaces were blackened by exposing them to the combustion gases of the engine chamber. Based on this assumption, no corrections for reradiation and reflection of radiation were made.

The calibration procedure consisted of exposing the heat flux probes to known, steady-state levels of radiant heat flux and measuring the corresponding temperature difference [ $T(0) - T(\delta)$ ]. With this procedure the quotient  $K/\delta$  is evaluated, since neither the thermal conductivity of the probe material  $K$  nor the distance of the "in-depth" thermocouple is precisely known.

**Measurements.** At each operating condition, after the engine was completely warmed and operating at steady state, the temporal variations of pressure in the main chamber and surface temperatures at three locations on the cylinder head (mostly at locations TM1, TM2 and TS1) were recorded for 100 consecutive cycles. From the transient surface temperature measurements and the corresponding temperatures of the "in-depth" thermocouples, the variation of heat flux during the engine cycle was calculated at each location.

Tests were performed for a wide range of engine speed (1000 to 3000 r/min), fuel-air ratio (0 to 0.040), and start of combustion (TDC to 10° ATDC) using No. 2 diesel fuel. The start of combustion was determined using a flame-luminosity probe located in the glow-plug position. The baseline conditions are shown in Table 2.

**Results and Discussion**

**Surface-Temperature Measurements.** Figures 2 and 3 show the temporal variations of the surface temperatures at TM1<sup>1</sup>

<sup>1</sup>The designations of the location of the probe, the probe itself, and the temperature at that location are identical.

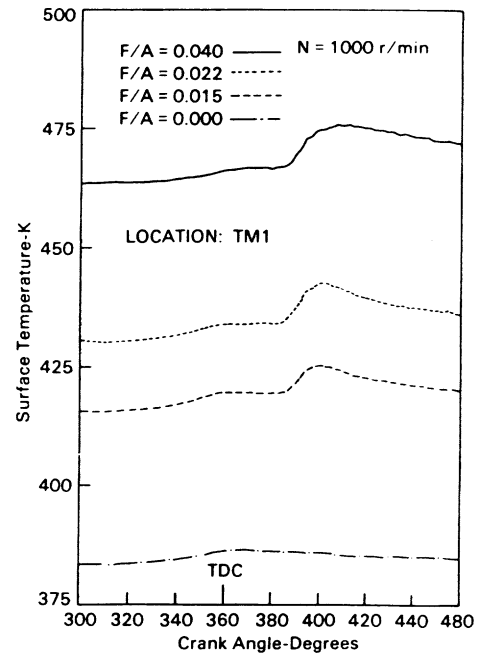


**Fig. 2 Temporal variations of the surface temperature at TM1 for various loads and an engine speed of 1000 r/min**

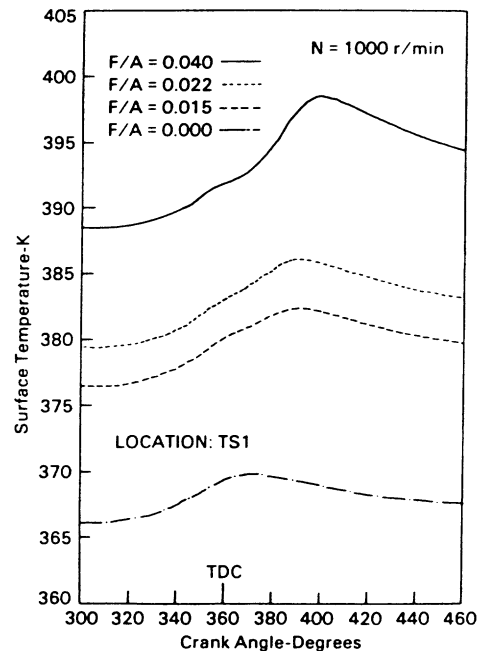


**Fig. 3 Temporal variations of the surface temperature at TS1 for various loads and an engine speed of 1000 r/min**

and TS1, respectively, for different fuel-air ratios and an engine speed of 1000 r/min during the time interval in the compression and expansion strokes of 60° BTDC (300° CA) to 100° ATDC (460° CA). As demonstrated in both figures, increasing the fuel-air ratio increased the overall surface temperature level and increased the temperature swing. At full load, the temperature swing during the engine cycle was about 10°C. An interesting point shown in Figs. 2 and 3 is that the peaks in the surface temperatures at locations TM1 and TS1 occurred later in the cycle as the fuel-air ratio was increased. This indicates that the combustion schedule of the fuel is retarded with increasing fueling rate. One should be reminded that the start of combustion (combustion timing), unless otherwise stated, was kept fixed at TDC.

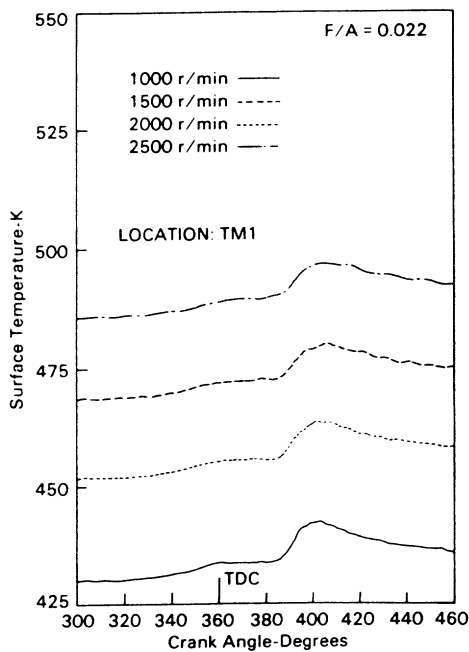


Fig. 4 Temporal variations of the surface temperature at TM1 for various engine speeds and a fuel-air ratio of 0.022

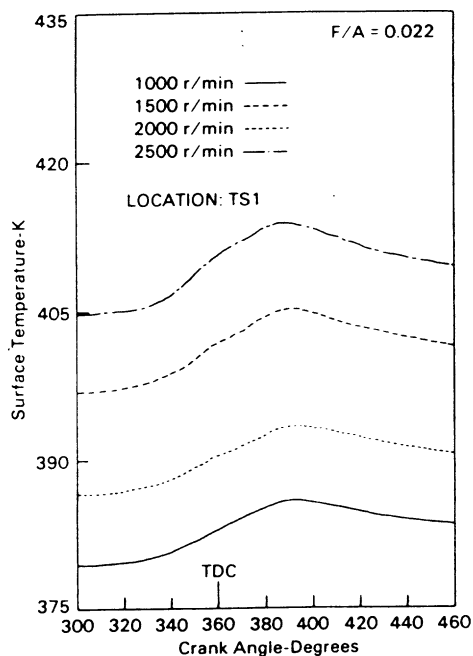


Fig. 5 Temporal variations of the surface temperature at TS1 for various engine speeds and a fuel-air ratio of 0.022

The temporal variations of surface temperatures at TM1 and TS1 for different engine speeds and a fuel-air ratio of 0.022 are shown in Figs. 4 and 5, respectively. Increasing engine speed increased the surface-temperature level. The temperature swing appears to be weakly influenced by engine speed.

**Surface Heat Flux Measurements.** In reciprocating internal combustion engines, the combustion-chamber surface heat flux may be represented by two components: the steady-state or time-averaged component, which can be evaluated from time-averaged temperature measurements at two known positions within the walls of the combustion chamber (e.g., see equation (1)), and the unsteady component, which can be

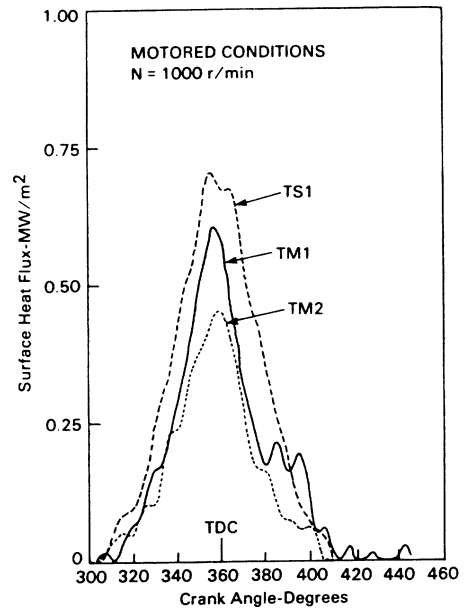


Fig. 6 Comparison of heat flux histories at TM1, TM2 and TS1 at motored conditions and an engine speed of 1000 r/min

evaluated from the measured cyclic surface-temperature variation.

The method of calculating the unsteady heat flux from transient surface-temperature measurements has been described in several studies [13-15]. Briefly, the measured cyclic surface-temperature variation is represented by a Fourier series of sine and cosine terms. The surface heat flux is then derived from the solution of the one-dimensional, unsteady heat-conduction problem with a time-varying surface temperature described by the foregoing harmonic analysis.

The method of calculating heat flux from temperature measurements (this includes the steady and unsteady components) assumes that the flow of heat in the combustion chamber walls is one-dimensional. In general, this is not true in engines [16]. However, the use of air gaps around the heat flux probes causes the flow of heat through the probes to be approximately one dimensional. Other errors associated with the measurement of heat flux in engines were discussed in [17].

A comparison of the temporal variations of the local heat fluxes at TM1, TM2, and TS1 for motored conditions and for an engine speed of 1000 r/min is shown in Fig. 6. The local heat fluxes peaked near TDC. Because of the high swirl flows present in the antechamber, the highest peak heat flux was measured at TS1, followed by the heat fluxes at TM1 and TM2. The observed spatial variations of the surface heat flux are primarily attributed to differences in the flow field in the vicinity of the measurements.

The influence of engine speed on the local heat flux history of TS1 is shown in Fig. 7 for motored conditions. Increasing the engine speed increased the characteristic velocity in the cylinder, which increased the convective coefficient and consequently the surface heat flux.

Comparison of the heat flux data for motored conditions obtained in this study with the corresponding data obtained by Kamel and Watson [11] showed that their magnitudes of the peak heat fluxes were higher by a factor of 2 to 4. This large difference in the measured heat flux level is primarily due to the difference in the magnitudes of the air velocities in the two combustion chambers and the difference in the locations of measurement of the two studies. The engine used by Kamel and Watson [11] had a Ricardo-Comet antechamber

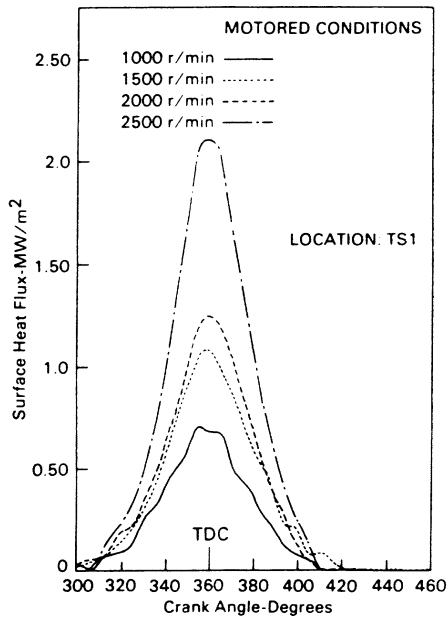


Fig. 7 The influence of engine speed on the heat flux history at TS1 (motored conditions)

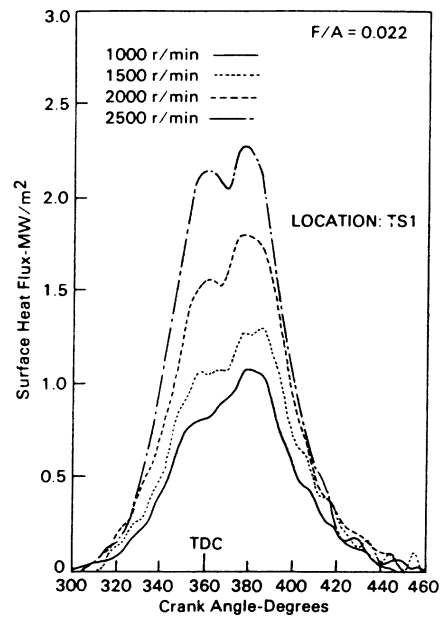


Fig. 9 Heat flux histories at TS1 for various engine speeds and a fuel-air ratio of 0.022

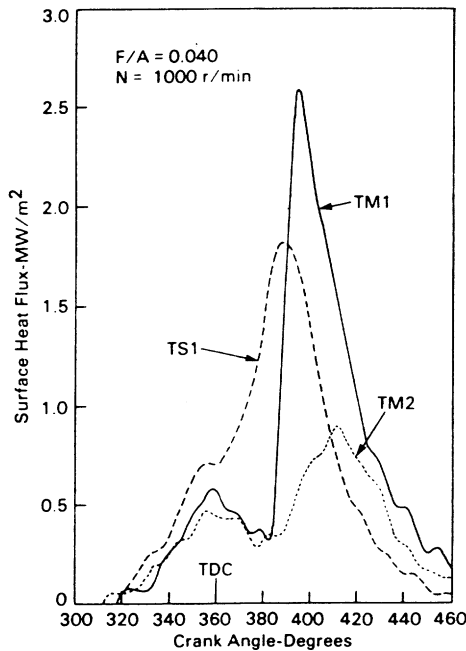


Fig. 8 Comparison of the heat flux histories at TM1, TM2 and TS1 for fuel-air ratio of 0.040 and an engine speed of 1000 r/min

that has a reported swirl ratio (angular velocity of air/angular speed of the engine crankshaft) of 20 to 70 [18, 19] with a more typical value of 40. In contrast, the engine used in the present study had a low-to-moderate swirl antechamber with swirl ratio of 10 to 20 [20, 21].

Comparison of the heat flux histories at TM1, TM2, and TS1 for an engine speed of 1000 r/min and fuel-air ratio of 0.040 is shown in Fig.8, respectively. As is apparent, the heat flux histories at fired conditions are characterized by double peak variations. The first peak, which in general is lower in magnitude, occurs near TDC (360° CA) and is due to compression (compression peak). The second peak, which occurs later in the cycle and is strongly dependent on location, is caused by combustion. In agreement with the heat flux measurements for motored conditions (e.g., see Fig.6), the

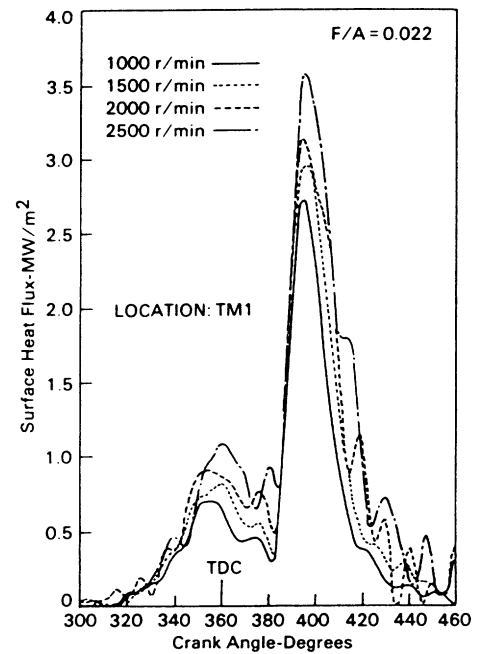
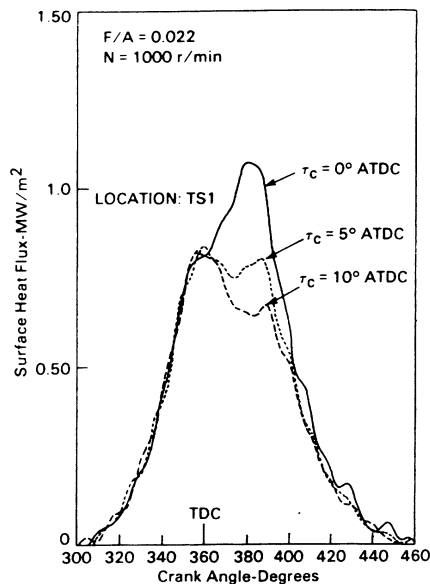


Fig. 10 Heat flux histories at TMI for various engine speeds and a fuel-air ratio of 0.022

peak heat flux due to compression was highest at TS1, followed by TM1 and TM2. On the other hand, in the case of the peak heat flux due to combustion, the highest heat flux was at TM1, followed by TS1 and TM2. Furthermore, in contrast to locations TS1 and TM2, the peak heat flux due to combustion at TM1 is several times larger than the corresponding peak heat flux due to compression.

It is apparent from Fig.8 that combustion affects the local surface heat flux histories significantly. The greatest influence of combustion is exhibited at TM1 because this location experiences the convective heating action of the hot combustion gases entering the main chamber from the antechamber during expansion. In relation to this, it is very interesting that the start of the second peak at location TM1 is



**Fig.11** The influence of combustion timing on the heat flux histories at TS1 ( $F/A = 0.022$ ,  $N = 1000$  r/min)

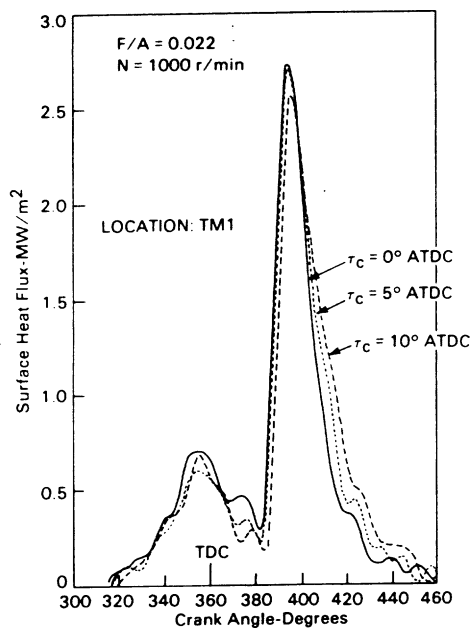


**Fig. 12** The influence of combustion timing on the heat flux histories at TM1 ( $F/A = 0.022$ ,  $N = 1000$  r/min)

well defined and occurs at about  $20^\circ$  CA ATDC. Thus one may conclude that TM1 senses the combustion gases entering the main chamber at about  $20^\circ$  CA ATDC. This has also been verified by luminosity measurements at the same location.

The effects of engine speed on the heat flux histories at locations TS1 and TM1 are shown in Figs. 9 and 10, respectively. All tests were run at a fuel-air ratio of 0.022 and the start of combustion at TDC. Increasing the engine speed significantly increased the heat flux levels at the two locations. However, the interval of high heat flux, expressed in crank angle degrees, appears to remain roughly constant. This suggests that the duration of combustion scales roughly inversely with engine speed.

A most interesting feature exhibited by the heat flux histories at TM1 is that the start of the second heat-flux peak

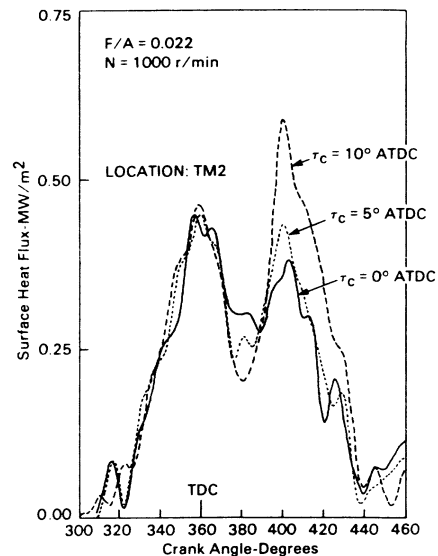


**Fig. 13** The influence of combustion timing on the heat flux histories at TM2 ( $F/A = 0.022$ ,  $N = 1000$  r/min)

and the initial stage of the rise in the heat flux due to combustion is independent of engine speed. This may suggest that the initial stage of outflow of gases from the antechamber is not significantly affected by engine speed.

Figures 11-13 show the influence of combustion timing on the heat flux histories at locations TS1, TM1, and TM2. All tests were performed at an engine speed of 1000 r/min and a fuel-air ratio of 0.022. Retarding the combustion timing ATDC significantly decreased the peak heat flux due to combustion at location TS1. Retarding the combustion timing after TDC causes reductions in gas pressure and combustion temperature, which reduce the rate of heat transfer. The heat flux history at location TM1 in the main chamber is not significantly affected by combustion timing, even though retarding the combustion timing decreased the peak heat flux due to combustion and retarded the heat-flux history due to combustion experienced by TM1.

In contrast to the results at TM1, the peak heat flux due to combustion at TM2, the other main-chamber location, increased significantly with retarded combustion timing. The observed different behaviors of the heat flux histories at locations TS1 and TM2 with combustion timing suggest that as the combustion timing is retarded, a proportionally larger amount of unburned fuel enters the main chamber, where it mixes and burns. The increase in the amount of fuel that burns in the main chamber causes the observed increase in the surface heat flux with retarded combustion timing.

## Conclusions

Transient surface heat flux measurements were performed at several locations on the cylinder head of a single-cylinder, divided-chamber diesel engine. The operational parameters of the engine examined and their ranges were: engine speed (1000 to 3000 r/min), fuel/air ratio (0 to 0.040), and combustion timing (TDC to  $10^\circ$  ATDC). Based on the results of this investigation, the following conclusions were reached:

- 1 The time histories of the local heat fluxes were significantly different at the three locations of measurement. These differences are attributed to the spatial nonuniformity of the fluid motion and combustion.

- 2 For motored conditions, due to the high swirl flows present, the highest heat flux was measured in the antechamber.

3 For fired conditions, the highest heat flux levels were measured at the location in the main chamber between the valves and in line with the throat of the antechamber. These high heat fluxes were attributed to the convective action of the high-temperature combustion gases exiting the antechamber during the early stages of the expansion stroke.

4 Both local time-averaged and local peak heat fluxes decreased with decreasing speed and load. Retarding the combustion timing beyond TDC decreased the peak heat flux in the antechamber but increased the peak heat flux in the main chamber. This is attributed to the relative increase in the portion of fuel that burns in the main chamber with retarded combustion timing.

In closing, one should be cautioned that, because of the extreme difficulties associated with the estimation of errors in the measurement of surface heat flux in the combustion chamber of a diesel engine, no error analysis of the heat flux measurements presented in this study was performed.

### Acknowledgment

The authors would like to acknowledge the efforts of L. E. Robb, who provided the main technical support to the experimental program.

### References

1 Sitkei, G., "Beitrag zur Theorie des Wärmeüberganges im Motor," *Konstruktion*, Vol. 15, 1962, pp. 67-71.

2 Annand, W. J. D., and Ma, T. H., "Instantaneous Heat Transfer Rates to the Cylinder Head Surface of a Small Compression-Ignition Engine," *Proc. Instn. Mech. Engrs.*, Vol. 185, 1971, pp. 976-987.

3 LeFeuvre, T., Myers, P. S., and Uyehara, A. O., "Experimental Instantaneous Heat Fluxes in a Diesel Engine and Their Correlation," SAE Paper 690464, 1969.

4 Whitehouse, N. D., "Heat Transfer in a Quiescent Chamber Diesel Engine," *Proc. Instn. Mech. Engrs.*, Vol. 185, 1971, pp. 963-975.

5 Oguri, T., and Inaba, S., "Radiant Heat Transfer in Diesel Engines," *SAE Transactions*, Vol. 81, 1972, pp. 127-148.

6 Dent, J. C., and Suliaman, S. L., "Convective and Radiative Heat Transfer in a High Swirl Direct Injection Diesel Engine," *SAE Paper 770407*, 1977.

7 Sibling, K., and Woschni, G., "Experimental Investigation of the Instantaneous Heat Transfer in the Cylinder of a High Speed Diesel Engine," Paper 790833, *Diesel Engine Thermal Loading*, SAE SP-449, 1979, pp. 95-103.

8 Knight, B. E., "The Problem of Predicting Heat Transfer in Diesel Engines," *Proc. Instn. Mech. Engrs.*, Vol. 179, 1965, pp. 99-112.

9 Hassan, H., "Unsteady Heat Transfer in a Motored I.C. Engine Cylinder," *Proc. Instn. Mech. Engrs.*, Vol. 185, 1971, pp. 1139-1148.

10 Kamel, M., "Thermodynamic Analysis of Indirect Injection Diesel Engine Operation," Ph.D. thesis, Imperial College of Science and Technology, University of London, 1977.

11 Kamel, M., and Watson, N., "Heat Transfer in the Indirect Injection Diesel Engine," Paper 790826, *Diesel Engine Thermal Loading*, SAE SP-449, 1979, pp. 81-94.

12 Bendersky, D., "A Special Thermocouple for Measuring Transient Temperatures," *Mechanical Engineering*, Vol. 75, No. 2, 1953, pp. 117-121.

13 Overbye, V. D., Bermethum, J. E., Uyehara, O. A., and Myers, P. S., "Unsteady Heat Transfer in Engines," *SAE Transactions*, Vol. 69, 1961, pp. 461-494.

14 Wendland, D. W., "The Effect of Periodic Pressure and Temperature Fluctuations on Unsteady Heat Transfer in a Closed System," NASA Report CR-72323, Mar. 1968.

15 Alkidas, A. C., "Heat Transfer Characteristics of a Spark-Ignition Engine," *ASME JOURNAL OF HEAT TRANSFER*, Vol. 102, 1980, pp. 189-193.

16 Hohenberg, G. F., "Advanced Approaches for Heat Transfer Calculations," *Diesel Engine Thermal Loading*, SAE SP-449, 1979, pp. 61-79.

17 Alkidas, A. C., and Myers, J. P., "Transient- Heat-Flux Measurements in the Combustion Chamber of a Spark-Ignition Engine," *ASME JOURNAL OF HEAT TRANSFER*, Vol. 104, 1982, pp. 62-67.

18 Alcock, J. F., and Watts, R., "The Combustion Process in High-Speed Diesel Engines," Paper A7, CIMAC Colloquium, Wiesbaden, 1959.

19 Alcock, J. F., and Scott, W. M., "Some More Light on Diesel Combustion," *Proc. Instn. Mech. Engrs. (A.D.)*, No. 5, 1962, pp. 179-197.

20 Zimmerman, D. R., "Laser Anemometer Measurements of the Air Motion in the Prechamber of an Automotive Diesel Engine," SAE Paper 830452, 1983.

21 Ahmad, T., Myers, J. P., and Groff, E. G., "Velocity Measurements in a Diesel Prechamber Using a Spark-Discharge Velocity Probe," submitted for presentation at the ASME Winter Annual Meeting, New Orleans, La., 1984.